氮对 316L不锈钢焊缝凝固模式和组织的影响

邓宝柱[1,2]， 马成勇[2]， 彭 云[1,2]， 田志凌[2]， 廖丕博[1]
（1. 昆明理工大学 机电工程学院，昆明 650093；2 钢铁研究总院 结构材料研究所，北京 100081）

摘 要：采用氮含量不同的三种焊丝分别对 316L奥氏体不锈钢进行了 TIG焊接，通过金相显微镜和扫描电镜对其焊缝微观组织进行了观察，对比分析了焊缝的凝固模式和焊缝组织的析出行为，研究了氮对焊缝凝固模式和组织的影响. 结果表明，焊缝氮含量为 0.018%时，焊缝的主要凝固模式为初生相为铁素体的 FA模式，δ铁素体以蠕虫状或网状分布于枝晶轴上；氮含量增加到 0.088%和 0.16%时，焊缝的主要凝固模式转变为初生相为奥氏体的 AF模式，δ铁素体以颗粒状分布于初生奥氏体枝晶间，其数目明显减少；焊缝奥氏体组织随着氮含量的增加有明显的粗化趋势.

关键词：氮；焊接；组织；凝固模式
中图分类号：TG115.28 文献标识码：A 文章编号：0253－360X(2010)05－0089－04

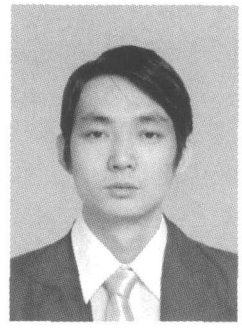

邓宝柱

0 序 言

316L奥氏体不锈钢具有良好的综合力学性能、耐腐蚀性能及焊接性能，因而广泛应用于各种石油化工及电站设备的生产制造中. 超低的碳含量保证了其优良的耐晶间腐蚀能力，但同时也显著降低了其强度，从而限制了 316L不锈钢在某些对强度要求较高的环境下的应用. 目前主要通过氮合金化来改善 316L不锈钢的强度，氮的固溶能明显提高其强度而不降低其它力学性能和耐腐蚀性能，氮还能有效抑制脆性 σ相的析出. 由于奥氏体的膨胀系数大而导热系数小，在奥氏体不锈钢焊接过程中，热裂纹是较易出现的主要问题之一，通常需要通过控制焊材成分和焊接工艺来促进焊缝以初生相为铁素体的铁素体－奥氏体模式（FA）凝固，并保证最终焊缝中存在 5%～12%的 δ铁素体来减小其热裂纹敏感性. 但有研究发现[1,2]，焊缝氮含量的增加显著增大了其热裂纹敏感性，这是由于氮具有强奥氏体化作用，在一定含量时能改变焊缝的凝固初生相从而改变其凝固模式和最终组织，焊缝的凝固模式和最终组织与其热裂纹敏感性有密切关系. 因而研究氮对焊缝凝固模式和组织的影响机理对于焊材和焊接工艺的合理选择至关重要. 文中采用不同含氮量的三种焊丝对 316L不锈钢进行了焊接，对比分析了三种焊缝熔敷金属的凝固模式和组织形态.

收稿日期：2008－12－15
基金项目：国防科工委年度项目

1 试验方法

母材为 316L不锈钢，三种焊丝均为自行研制，直径均为 φ2.4 mm，其熔敷金属化学成分分析结果如表 1所示.

表 1 熔敷金属的化学成分（质量分数，%）
Table 1 Chemical composition of weld metals

C	P	S	Cr	Ni	Mo	N	Fe
0.025	≤0.01	≤0.01	18～20	12～14	2.0～2.8	0.018	余量
0.016	≤0.01	≤0.01	18～20	12～14	2.0～2.8	0.088	余量
0.028	≤0.01	≤0.01	18～20	12～14	2.0～2.8	0.160	余量

试板尺寸及坡口设计参照国家标准 GB2652—89《焊缝及熔敷金属拉伸试验方法》，焊接工艺参数见表 2.

表 2 焊接工艺参数
Table 2 Welding parameters

电压 U/V	电流 I/A	焊接速度 v/(mm·s⁻¹)	保护气体	气体流量 q/(L·min⁻¹)	层间温度 T/℃
12	180	100	高纯氩	10	＜100

焊前试板及垫板均用钢丝刷进行表面清理. 试验过程中采用 AMET Manipulator焊机对控氮 316L不锈钢进行 TIG焊接. 金相试样经打磨抛光，在 10%铬酸中电解约 30 s，电压为 4.5 V. 采用 LEICA MEF4金相显微镜和日本 HITACHI S-4300型扫描

电镜(SEM)对焊缝最后焊道组织进行观察,采用扫描电镜上配带的能谱仪(EDAX)进行成分分析;采用铁素体磁性测量仪对焊缝不同位置的铁素体含量进行了测量;参照国家标准 GB2649—89《焊接接头机械性能试验取样方法》截取了焊缝的拉伸及冲击试样,试验分别在 UH—F50A(250 kN)拉伸试验机和 JBZ—300自动冲击试验机上进行.

2 试验结果及分析

2.1 氮对焊缝凝固模式的影响

根据凝固初生相和最终组织的不同,可以将不锈钢焊缝的凝固模式分为 A,AF,FA和 F四类. Suutala等人[3]以 Cr_{eq}/Ni_{eq}的形式表达了焊缝凝固行为和成分因素如图 1所示的线性关系.

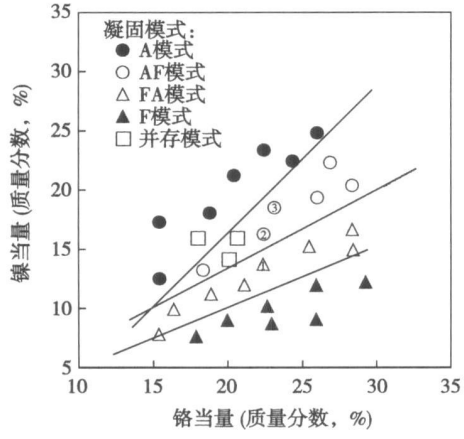

图 1 焊缝凝固模式和成分的关系

Fig. 1 Relationship between solidification mode and composition

图中对应初生相为奥氏体的 AF模式和初生相为铁素体的 FA模式分界线的 Cr_{eq}/Ni_{eq}约为 1.5.这个数值已被证明对于以常规焊接工艺焊接的 300多种合金是有效的[4].文中根据三种焊缝熔敷金属化学成分计算出的 Cr_{eq}/Ni_{eq}分别为 1.58,1.49和 1.40对应图 1中的 1,2,3三个位置,其凝固模式应该分别为 FA,AF和 AF.

奥氏体不锈钢焊缝的凝固模式可以通过其室温组织和 δ铁素体的形态来辨别.焊缝以 FA模式凝固时,初生相为铁素体,奥氏体在铁素体枝晶间析出,随后在固相冷却和铁素体数目(FN)减少的过程中向铁素体内部生长,如图 2a所示;焊缝以 AF模式凝固时,初生相为奥氏体,随后析出的 δ铁素体最终保留在奥氏体枝晶间,如图 2b,c所示.需要指出的是图 2b所示焊缝中部分区域仍存在 FA模式,这可能是由于其焊缝的 Cr_{eq}/Ni_{eq}接近临界值 1.5,且为整个焊缝的平均值,氮在焊缝中的分布不均匀,因而在局部贫氮的区域由于 $Cr_{eq}/Ni_{eq}>1.5$而出现 FA凝固模式.

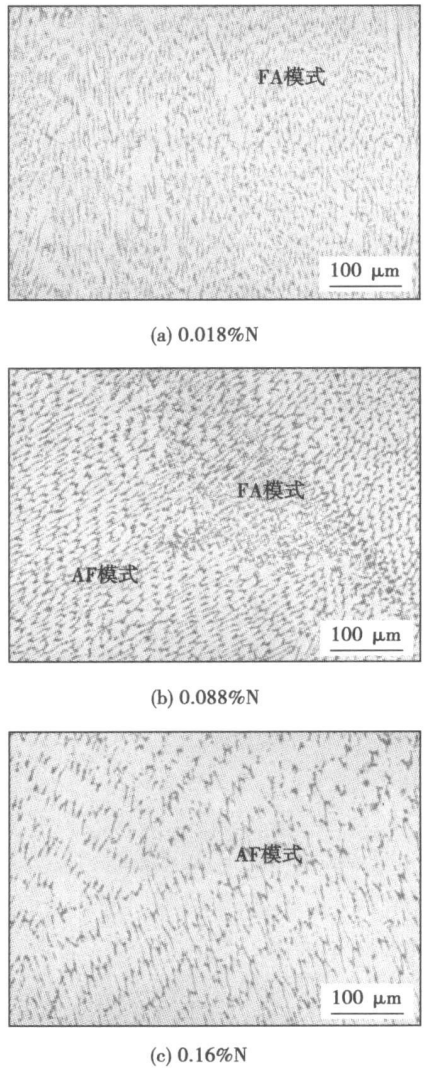

图 2 焊缝熔敷金属组织形貌

Fig. 2 Microstructure of weld metals

综上所述,氮对焊缝凝固模式的影响主要是因为其改变了焊缝的 Cr_{eq}/Ni_{eq},从而改变了焊缝凝固初生相.

从图 3所示的 65Fe-xNi-yCr合金系伪二元相图[5]中可以看出不同氮含量的三种焊缝的凝固过程.图中三条线分别标明了含氮量为 0.018%,0.088%和 0.16%的三种成分在伪二元相图中的位置,1号线表示的组织转变过程为 L→L+δ→L+δ+γ→δ+γ(FA模式);2号和 3号线表示的组织转变过程为 L→L+γ→L+δ+γ→δ+γ(AF模式).由

此得出的凝固模式与之前通过 Cr_{eq}/Ni_{eq}的计算分析和实际焊缝中观察到的凝固模式相吻合.

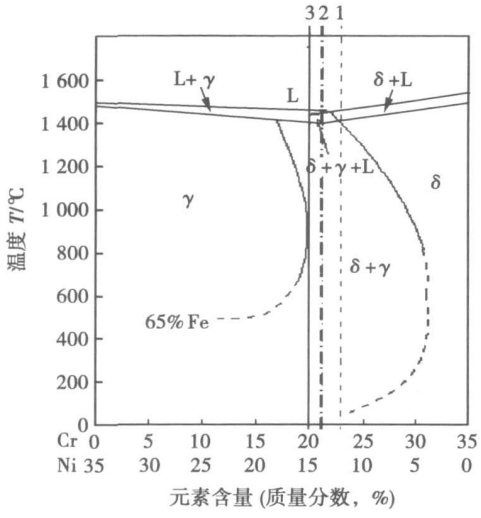

图 3　65Fe-xNi-yCr合金系伪二元相图

Fig. 3　Pseudo-binary diagram of 65Fe-xNi-yCr system

2.2　氮对焊缝组织的影响

氮是一种很强的奥氏体化元素，不仅能稳定奥氏体组织，对焊缝中铁素体的形态、数目和分布也有重要影响. 从图 4所示的焊缝组织的 SEM组织形貌来看，三种焊缝中的铁素体的形态、数目和分布都存在一定差别. 以 FA模式凝固的焊缝中，铁素体以蠕虫状和网状分布在富铬的枝晶轴上；而在以 AF模式凝固的焊缝中，残余的铁素体呈现小颗粒的形态分布在初生奥氏体枝晶间，铁素体数目随着含氮量的增加而减少.

文中通过计算和实测两种方法分析了三种焊缝的铁素体数目（FN）. 通过 Cr_{eq}/Ni_{eq}计算，再对照修正的舍夫勒组织图[6]得出焊缝的 FN分别为 8、3.5、1，见图 5；铁素体磁性测量仪的实测值分别为 7.6、3.2、1.1，可以看出随着含氮量的增加，焊缝 FN呈现如图 6所示的下降趋势.

焊缝中铁素体的形态、数目和分布对奥氏体组织的析出和长大行为有一定影响. 从图 2所示的焊缝显微组织可以看出，随着氮含量的增加，焊缝的奥氏体组织逐渐粗化，氮含量从 0.018%增加到 0.088%时粗化现象较为明显. 图 2a中 δ铁素体主要以蠕虫状分布于枝晶主轴上，凝固过程中阻碍了奥氏体柱状晶的长大. δ铁素体还具有强烈的形核效果，再结晶过程中，δ→γ转变形成细小的新奥氏体晶粒，阻碍了晶粒粗化，因此焊缝最终组织较为细小；图 2b、c焊缝中 δ铁素体主要分布于枝晶间，其数目也相对较少，而且在凝固后期产生，其细化柱状晶和形核效果都很小，因而焊缝最终的奥氏体组织相对粗大.

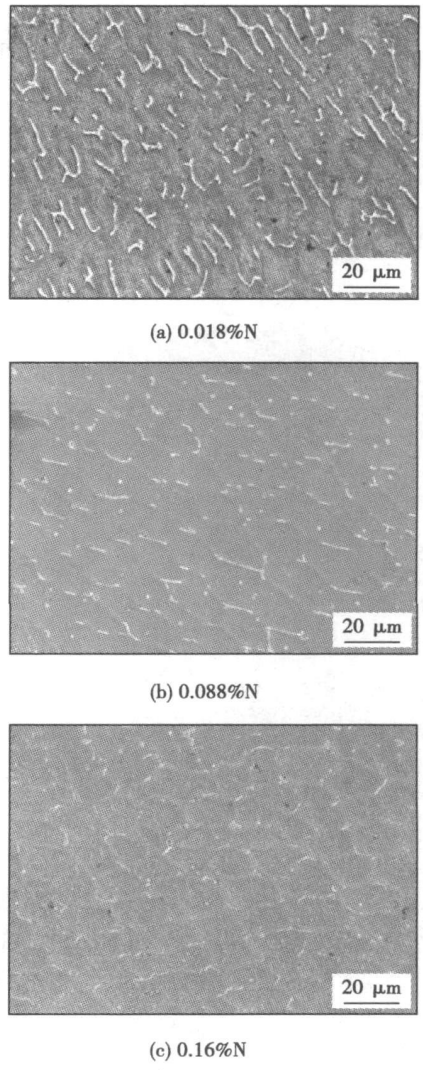

图 4　焊缝铁素体 SEM 组织形貌

Fig. 4　Ferrite morphology of weld by SEM

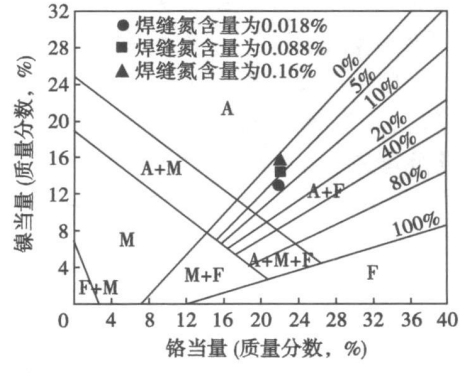

图 5　修正的舍夫勒组织图

Fig. 5　Modified shaeffler diagram

除了上述铁素体对奥氏体组织的影响，从枝晶

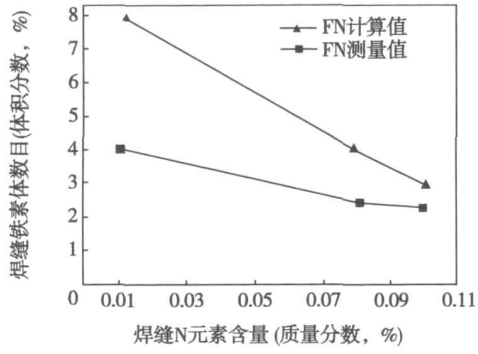

图 6 焊缝氮含量与铁素体含量关系

Fig. 6 Relationship between nitrogen content and ferrite number

本身来看，焊缝的一次枝晶间距 λ_1 和二元合金系凝固过程中的热循环及材料变量有关[7]，即

$$\lambda_1 = \frac{4.3(\Delta T_0 D\Gamma)^{0.25}}{(KR)^{0.25} G^{0.25}} \quad (1)$$

式中：ΔT_0 为凝固温度区间；D为溶质扩散系数；Gibbs系数 $\Gamma = (\sigma / \Delta S_f)$为固—液表面能与熔化熵之比；K为平衡溶质分配系数；R为凝固速度；G为温度梯度．在其它变量都相同的情况下，$\Delta T_0 = mC_0(1-k)/k$ 其中 m为液相线斜率；C_0 为溶质元素在液体中的初始固溶量．通过这个等式可以将一次枝晶间距公式写成与固溶量相关的简化形式，即

$$\lambda_1 = A(C_0)^{0.25} \quad (2)$$

式中的常数 A综合了除固溶量 C_0 以外的其它因素，可以看出，枝晶间距随氮含量的增加而增加，宏观上表现为枝晶的粗化．

根据上述分析，氮对 316L不锈钢焊缝的凝固模式和组织都有影响．有研究发现，在不同凝固模式下，氮对不锈钢焊缝强度的影响程度不同，此外 δ铁素体数目的变化也会直接影响焊缝的力学性能[8]．文中试验最后对三种焊缝的拉伸及冲击性能分别进行了试验分析，结果发现，随着氮含量的增加，焊缝的抗拉强度明显提高，但其断后伸长率有所下降，冲击韧性没有明显变化．

3 结 论

(1) 焊缝氮含量由 0.018%增至 0.088%和 0.16%时，焊缝的凝固模式发生了由 FA至 AF的转变．

(2) 焊缝氮含量的增加导致了焊缝铁素体形态、数目和分布的变化．

(3) 随着焊缝氮含量的增加，焊缝奥氏体组织呈现粗化趋势．

参考文献：

[1] Lin Y C, Chen P Y. Effect of nitrogen content and retained ferrite on the residual stress in austenitic stainless steel weldments [J]. Materials Science and Engineering A, 2001, 307(1/2): 165—171.

[2] Shankar V, Gill T P S, Mannan S L, et al. Effect of nitrogen addition on microstructure and fusion zone cracking in type 316 stainless steel weld metals [J]. Materials Science and Engineering A, 2003, 343(1/2): 170—181.

[3] Suutala N, Moisio T. Solidification technology in the foundry and casthouse [M]. London: The Metals Society, 1980.

[4] Vasudevan M, Bhaduri A K, Baldev R, et al. Artificial neural network modeling of solidification mode in austenitic stainless steel welds [J]. Materials Science and Technology, 2007, 23(4): 451—459.

[5] Sedriks A J. Corrosion of Stainless Steels [M]. New York: Wiley & Sons, 1979.

[6] Schaeffler A L. Constitution diagram for stainless steel weld metal [J]. Metal Progress, 1949, 56(11): 680—688.

[7] Kurz W, Fischer D J. Fundamentals of Solidification [M]. New York: Trans Technology, 1985.

[8] Deepashri D N, Raja V S. Effect of nitrogen addition on the microstructure and mechanical behavior of 317L and 904L austenitic stainless steel welds [J]. Journal of Materials Science, 2006, 41(7): 2097—2112.

作者简介：邓宝柱，男，1983年出生，硕士．主要从事不锈钢焊接方面的科研工作．发表论文 1篇．

Email: danny_9527@163.com

model was developed in order to investigate the temperature and flow fields in a free burning TIG arc. A series of arc models were founded. The different flow and temperature fields of the arc in different flow rates and different arc lengths were calculated and compared. With the increase of arc length, the temperature of arc, the arc voltage and the flow velocity are increased. But the velocity stabilized in a certain value when the arc length is 8-10 mm. The moderate arc length can assure the arc with optimal heat input and better protection. The increased flow rate of shielding gas compresses the arc and causes the energy emission to be much closer to the axis center, and the highest temperature is also increased. With the flow rate further increases, the energy emission and heat transfer increase, the highest temperature declines. The anticlockwise swirl streamtraces become larger as the flow rate increases and govern the arc region, thus the quality of flow protection is improved. The area of higher velocity in the arc column has left the original position and moved to the electrode. But the higher flow rate will delay the radial velocities on the anode.

Key words: arc; numerical simulation; flow rate; arc length

Brazing of C_f/SiC composite to Ti alloy with Ag-Cu-Ti-C_f composite filler XIONG Jinhui, HUANG Jihua, ZHANG Hua, ZHAO Xinke (School of Materials Science and Engineering, University of Science and Technology Beijing, Beijing 100083, China). p 77 - 80

Abstract: C_f/SiC was successfully joined to Ti alloy with Ag-Cu-Ti-C_f (C_f, carbon fiber) mixed powder by proper brazing parameters. Microstructure of the brazed joints were investigated by SEM, EDS and XRD. Its mechanical properties were measured by mechanical testing machine. The results showed that Ti element in the interlayer can react with the brazed composite, a mixture of Ti_3SiC_2, Ti_5Si_3 and TiC composites finally formed in the reaction layer between composite and interlayer. Ti alloy constantly dissolves and Cu diffuses into the Ti alloy, which forms the diffusion-reaction layers between interlayer and Ti alloy. The performed joints have dense bonding layers reinforced by short carbon fibers. These composite in brazing layers relaxes the thermal stress of the joints effectively. The shear strength of the joint brazed with Ag-Cu-Ti-C_f filler was remarkably higher than that with pure Ag-Cu-Ti filler.

Key words: C_f/SiC composite; Ti alloy; brazing

Numerical simulation on temperature field of laser cladding based on birth-death element method ZHAO Hongyun, SHU Fengyuan, ZHANG Hongtao, YANG Xianqun (School of Materials Science and Engineering, Harbin Institute of Technology at Weihai, Weihai 264209, Shandong, China). p 81 - 84

Abstract: The temperature increase of powder particles was computed with different laser power as the main parameter, and it was used as an initial condition in analyzing temperature field of both single and multiple laser cladding with birth-death element method. The reliability of the model was verified by the dimension and morphology of the molten pool. The temperature of particles increases linearly with laser power being increased. The temperature curve of single clad shows a sawtooth type, in which the temperature increases linearly and decreases as half of a hyperbolic curve. The temperature field of multiple cladding shows a backward dragged ellipse. The thermal cycle of every node goes though some several incremental peaks and tends to a stable state in the end.

Key words: laser cladding; birth-death element method; temperature field; initial condition

Prediction of fatigue life based on change of natural frequency and load characteristic for spot welded joint LI Xuepeng, SHANG Deguang, ZHOU Jianwei, BAO Ming (College of Mechanical Engineering and Applied Electronics Technology, Beijing University of Technology, Beijing 100124, China). p 85 - 88

Abstract: By the fatigue experiment and dynamic response experiment, the variation characteristic of natural frequency was investigated based on the single tensile-shear spot-welded specimens during the fatigue process with constant amplitude, variable amplitude and random loading. Frequency response function curve and modal natural frequency were compared during the fatigue process in this paper. According to the rates of frequency change and the residual life ratio, a fatigue parameter was proposed to describe the fatigue process under random loading, and a linear relationship was established between the rate of frequency change and the fatigue parameter. The fatigue life was predicted on the basis of loading spectrum, the rate of frequency change and current cycle number. The proposed method can be used in the situation that loading spectrum was given and natural frequency was measured. The calculated results showed that the predicted fatigue lives were in good agreement with experimental lives.

Key words: spot welding; dynamical response; natural frequency; fatigue; life prediction

Effect of nitrogen on solidification mode and microstructure of 316L stainless steel DENG Baozhu[1,2], MA Chengyong[2], PENG Yun[1,2], TIAN Zhiling[2], LIAO Pibo[1] (1. Faculty of Mechanical and Electrical Engineering, Kunming University of Science and Technology, Kunming 650093, China; 2. Institute of structural Materials, Central Iron & Steel Research Institute, Beijing 10081, China). p 89 - 92

Abstract: Three kinds of welding wires with different nitrogen contents were used for TIG welding of 316L austenitic stainless steel. The solidification mode of the welds and the precipitation behavior of austenite and ferrite were contrastively analyzed, and the effect of nitrogen on solidification mode and microstructure of the weld metal was investigated. The results show that the weld with nitrogen content of 0.018% solidifies as primary ferrite mode and vermicular or skeletal ferrite remains on the dendritic axis. With the increase of nitrogen content to 0.088% and 0.16%, the weld solidifies as primary austenite mode and ferrite occurs as small particles between primary austenite dendrites; the ferrite number (FN) decreases and the remarkably coarse austenite is also found.

Key words: nitrogen; welding; microstructure; solidification mode